Macromolecules
ARTICLE

Macromolecules **2009**, *42*, 7877–7880 **7877**
DOI: 10.1021/ma901321k

Moisture Effects on *Antheraea pernyi* Silk's Mechanical Property

Chengjie Fu,[†] David Porter,[‡] and Zhengzhong Shao*,[†]

[†]*Key Laboratory of Molecular Engineering of Polymers of Ministry of Education, Advanced Materials Laboratory, Department of Macromolecular Science, Fudan University, Shanghai 200433, P.R. China, and* [‡]*Department of Zoology, University of Oxford, South Parks Road, Oxford OX1 3PS, United Kingdom*

Received June 30, 2009; Revised Manuscript Received August 26, 2009

ABSTRACT: Water plays an essential role in determining the mechanical properties of silks and other structural proteins. Here we study the effects of moisture on the elastic modulus of *Antheraea pernyi* silks, which exhibit an abrupt drop over a narrow range of relative humidity in the same way as synthetic polymers do in a temperature scan through their glass transition. A linear relationship between relative humidity and the transition temperature allows a simple transformation of the modulus−humidity curves into a general modulus−temperature relation for *Antheraea pernyi* silks. A model is presented to explain these observations quantitatively at the molecular level.

1. Introduction

Natural silks are a family of structural materials with an attractive balance of modulus, strength, and toughness.[1,2] The relatively high elastic modulus of silks is due to the high density of inter- or intrachain hydrogen bonds between the polar amide groups, which does however make silks vulnerable to water molecules. The usual result of treating silks with water or moisture is the reduction of stiffness by up to an order of magnitude and a noticeable increase in elongation to break.[3−6] For example, the dragline silk of *Nephila clavipes* (*N. clavipes*) with an average initial modulus of 13.7 GPa and breaking elongation of 22.6% at 25% relative humidity (RH) turns into a more compliant fiber with an average initial modulus of 1.4 GPa and breaking elongation of 39.8% after exposure to the environment of 80% RH.[5] Such large variations in mechanical properties can be attributed to the activation of the glass transition of silk protein chains in the presence of water. Though the closely packed crystal structure is immune to water, the disordered regions (or amorphous regions) in silks are quite accessible to water, which disrupts the amide−amide hydrogen bonds and improves the mobility of protein chains within these regions, i.e., plasticizes these regions.[7−11] DSC results revealed that moisture-containing (∼5%) amorphous films of *Bombyx mori* (*B. mori*) silk fibroin have a low-temperature glass transition at about 60 °C, in comparison to the glass transition temperature (T_g) of 178 °C for dry films.[11] Agarwal and co-workers reported the gradual reduction of the T_g of amorphous *B. mori* silk fibroin films with increasing moisture content, which was in general agreement with the semiempirical Couchman and Karasz expression.[12] Plaza and co-workers showed that the T_g of spider dragline silk decreases with increasing relative humidity by monitoring the tensile modulus and supercontraction degree of the silk under systematically varying temperatures and humidities.[13] However, their method uses a large number of samples, which limits the accuracy of the results, as variability among biomaterial samples is unavoidable. Also, in their method, the modulus variation with the humidity is actually determined by two factors: moisture content in the sample and the degree of orientation or order in the sample. Since the latter changes when supercontraction occurs at elevated humidity, this makes the relationship between modulus and moisture content ambiguous.

The water-plasticizing phenomenon not only is found in silks but also is a controlling factor in the mechanical properties of most structural proteins that usually function under highly hydrated conditions *in vivo*, such as collagen and elastin. It is also an important effect that is found in synthetic polymers with hydrophilic groups, such as nylons and epoxy resins.[14−16] For example, a shift in T_g of more than 80 °C can be observed by increasing the moisture content from dry nylon-6 to that conditioned at 92% humidity.[15] For a lightly cross-linked epoxy resin, T_g reduction of 13−15 °C with each wt % water content was reported.[16] Therefore, studying the moisture effects on the mechanical properties of animal silks is of more general importance as it provides us a useful insight into structure−property relationships in the polymers with hydrophilic groups.

Here, by using an individual fiber, we systematically studied the moisture effect on the modulus of the *Antheraea pernyi* (*A. pernyi*) silk (a kind of wild silkworm silk) under different temperatures. From the modulus−relative humidity curve, a critical humidity was identified as the onset point where the modulus begins to drop sharply with increasing humidity. Then the experimental temperatures were plotted against the relevant critical humidities, so that the effects of humidity on the T_g of disordered regions in the *A. pernyi* silk can be quantified. With such knowledge, we derived a general modulus−temperature master curve which demonstrates a clear identity between humidity and effective temperature in the silk relative to the T_g with zero moisture. These experimental observations then provided an ideal starting point for explaining the effect of water on the mechanical properties of animal silks using a relatively straightforward molecular level model.

2. Experimental Section

Silk Preparation. Silks were forcibly reeled at 8 mm/s from the mature larval of *A. pernyi* silkworm which previously lived on the oak trees in a tussah field of Shandong province, China. The silk was first contracted without constraints in water (the contraction was around 5%) for about 0.5 h and then dried in air. Such a process did not remove all the coated sericin which could be observed by SEM (see Figure SI1). The thickness of

*Corresponding author. E-mail: zzshao@fudan.edu.cn.

Published on Web 09/11/2009

sericin residue was about 200−300 nm, while a single brin of the *A. pernyi* silk was about 16−17 μm. We did not take the sericin into account in the discussion below mainly because it was small amounts in such a case and worked as a very hydrophilic coat which might rarely contribute to the modulus of the moist fiber, although the real effect of sericin coat on the properties of silk was hardly known. Water contracted silk was used here instead of as-reeled sample, as water contraction eliminates the influence of orientation degree on the mechanical properties of silk, leaving the moisture content as the only variable. A single silk thread (a bave) 10 mm long was adhered onto a frame made from aluminum foil with cyanoacrylate super glue. An extra layer of nail varnish was brushed on the adhering point to prevent moisture from deteriorating the adhesive effect of the super glue.

Loading−Unloading Test. The sample was held unstrained on the clamps of an Instron 5565 and equilibrated for at least 0.5 h under the required temperature and humidity in the environmental chamber, which was integrated with the Instron 5565. A loading−unloading program was applied to the sample with a maximum strain of 0.6% at 0.001 s^{-1} strain rate. A small strain of 0.6% was applied to avoid permanent deformation of the sample. The repeatability of the experiment was checked with the sample used and its neighboring sample (data not shown); no noticeable deviation was found. Because of the small dimension of the silk fiber, sawtoothed noise was observed in the load−strain curves (Figure 1A). It is caused by disturbance of the cycle current in the environmental chamber. At least five loading−unloading tests were performed for each relative humidity at any given temperature. It should be noted that the results of the test were repeatable for the fibers reeled from different larval, and the typical one was presented.

Cross-Sectional Area Measurement. The cross-sectional area of the silk was estimated by analyzing the transverse fracture face of silk-embedding epoxy resin under Tescan 5136MM. The image was obtained by using back scattering electrons at 10 kV. With the cross-sectional area, the load−strain curves were changed to stress−strain curves, from which the modulus of silk was calculated.

Dynamic Mechanical Analysis (DMA). The ends of the silk were first clamped between two layers of hard paper board, which were then fixed on the film tensile clamp of TA Q800 DMA. The test was preformed at 1 Hz with a temperature ramp rate of 3 °C/min.

3. Results and Discussion

To avoid permanent deformation of the sample, a small strain of 0.6% was employed during the loading−unloading test (the yield point of such silk is around 2.4% of strain). Therefore, it allows us to measure the change of modulus over a wide range of humidity and temperature with just one sample since the structure of silk is not destroyed in the cycles.

As shown in Figure 1A, the slope of load−strain curves does not change evenly as the relative humidity increases. This trend is more obvious in Figure 1B, where moduli begin to fall rapidly at a critical humidity (onset point of transition for an individual curve is shown in Figure 1C) after showing little change at the low humidity levels. Take the data at 25 °C for instance; the modulus of the *A. pernyi* silk gradually decreases from 11.8 GPa at 10% RH to 8.5 GPa at 70% RH, from which it drops to 0.8 GPa at 98% RH. The transition point shifts to lower relative humidity at higher temperatures. For example, the transition point in relative humidity reduces from 80% RH to 51% RH when the temperature increases from 10 to 85 °C. This observation coincides with the findings with spider silk in the literature, and even the critical humidity values are similar.[13]

An interesting feature in Figure 1A is that the hysteresis loop between the loading and unloading curves becomes most obvious around the critical humidity. Since the area of the hysteresis loop

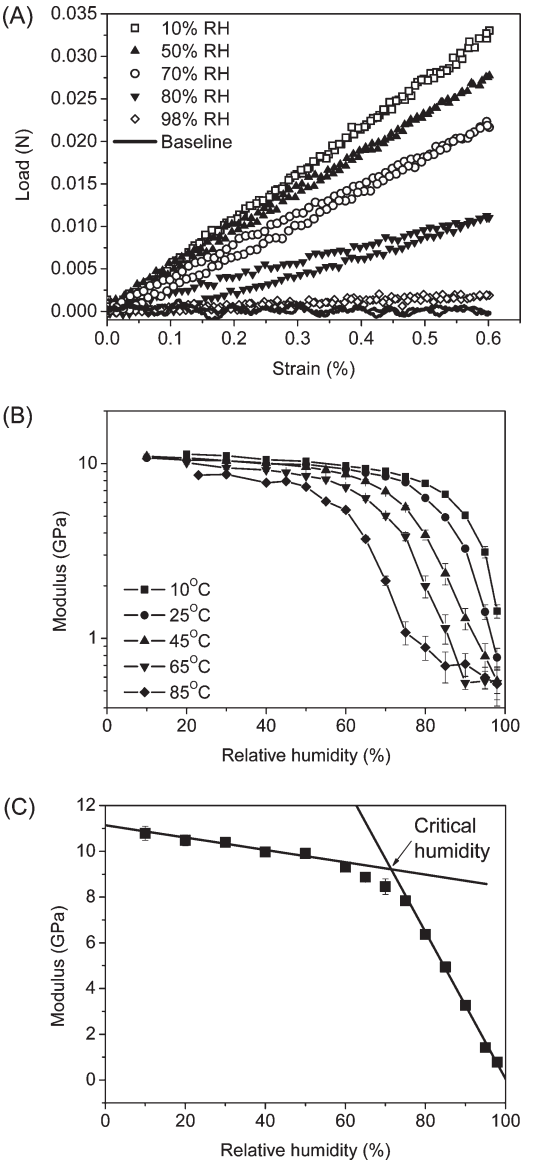

Figure 1. (A) Load−strain curves of water contracted *A. pernyi* silks at 25 °C at different humidities; the baseline was obtained by an loading−unloading experiment with no sample on the clamps of the Instron. (B) Modulus−relative humidity curves at five different temperatures; each point is the average result of five tests and is shown with error bar. (C) Definition on the critical humidity in the modulus−relative humidity curve at 25 °C.

indicates the energy dissipated during the loading−unloading cycle, the observation means the silk is most energy-dissipative around the critical humidity. This behavior is similar to that observed in traditional polymers around their own characteristic temperature, i.e., T_g. Under temperatures far below T_g, the macromolecular chains are immobile, such that only the elastic response of the chains is observed with little energy dissipation. Conversely, at temperatures far above T_g, the frictional force between chain segments is so low that they move with little energy dissipation. Around T_g, energy dissipation, as measured by properties such as loss tangent in DMA, goes through a massive peak. Therefore, it appears reasonable to assign the critical humidity as the glass transition condition at the temperature of measurement or, conversely, assign the temperature of measurement as the T_g at the critical humidity.

By plotting the temperature against the critical relative humidity obtained in Figure 1B, a linear relationship is shown in

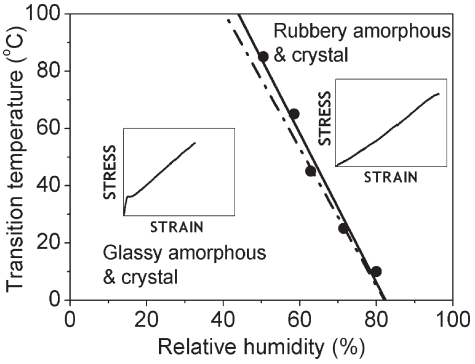

Figure 2. Linear relationship between the relative humidity and transition temperature. The solid line is a best fit [$T_g = 214 - 2.6H$ ($R = 0.99$)], and the dash-dotted line is predicted by the GIM model ($T_g = 197 - 2.4H$) explained in the text for detail, where T_g is the transition temperature and H is relative humidity. Left inset is the representative stress−strain curve of water contracted *A. pernyi* silk tested at 20 °C, 50% RH; right inset is the representative stress−strain curve of water contracted *A. pernyi* silk tested in water at 25 °C.

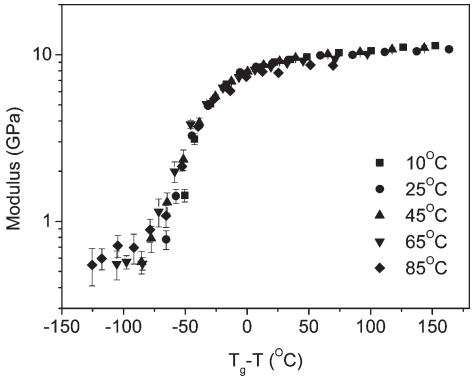

Figure 3. General modulus−(T_g−T) master curve for *A. pernyi* silk. The T is the temperature of measurement, and T_g is the virtual glass transition temperature dependent on relative humidity in measurements.

Figure 2 (the solid line). Extrapolating the line to 0% RH yields a transition temperature of 214 °C, in good agreement with previous DMA results carried out with both *A. pernyi* silk fibroin film[17] and fiber (refer to Figure 4 as shown below). At the opposite extreme, extrapolating the line to 100% RH yields a transition temperature of −48 °C, which means the amorphous regions in the silk are rubbery at high humidity. Such a glass−rubber transition in the amorphous region is illustrated with two insets in Figure 2 on either side of the transition condition.

The linear relationship indicates an equivalence between relative humidity and temperature in affecting the properties of silk. The water fraction absorbed by the disordered regions of silk is proportional to the relative humidity when the humidity is neither too low nor too high (for example, between 20% RH and 80% RH),[12] although this must be investigated in more detail in future work. We therefore deduce that the extra thermodynamic degrees of freedom of the more mobile water molecules are increasing the thermal energy in the protein in a way that is linearly equivalent to increasing the temperature. Since the glass transition is an isoenergetic state, this means that higher humidity must have a lower temperature at which the condition is satisfied.

With the linear relation between temperature and relative humidity, the humidity effects on modulus can be transformed into temperature effects according to the fitted equation $T_g = 214 - 2.6H$. In this way, we can plot a general modulus−(T_g−T) curve for *A. pernyi* silks, as shown in Figure 3 by "merging" five curves at different temperatures into a single master curve. This process is comparable to forming master curves from DMA tests on synthetic polymers. The dependence of mechanical properties on the difference between experimental temperature and the primary relaxation temperature is also observed in nylon-6.[15] With the same temperature difference, nylon-6 tested under widely separated temperatures shows very similar yielding and strain-hardening behaviors.

In order to explain the observed relationship between elastic modulus, T_g, and humidity in *A. pernyi* silk, we have used structure−property relations for polymers that have been applied successfully to silks to predict mechanical properties as a function of temperature. The model framework is called group interaction modeling, GIM, and is documented in detail for synthetic polymers to predict their highly nonlinear viscoelastic properties as a function of temperature, strain, and strain rate.[18,19] Application of the model to silks has shown that the mechanical properties of any silk can, in principle, be predicted from its composition and fraction of "order", which is loosely identified with crystal fraction;[20−22] the model is presented in more detail in the Supporting Information for reference. For this work, we start from predictions of elastic modulus through T_g in the dry silk and then change the temperature scales to account for the effect of humidity.

A recent paper has discussed the interaction of water with the protein chain backbone in some detail and suggested that the equilibrium fraction of absorbed water is proportional to the relative humidity of the environment and that this fraction is determined by two water molecules being able to hydrogen bond to the chain amide group in each peptide segment.[23] Thus, the limiting molar fraction of bound water per peptide segment at 100% RH is 0.67.

The T_g of the dry silk is taken to be the relevant observed value of 470 K (197 °C) at the crossing point of lines extended from the elastic modulus curve above and below T_g; this is a pragmatic approach to quantifying T_g, since the same method can be used for plots of modulus as a function of humidity. The GIM predicted value of 491K (218 °C) for the amide segment using the loss tangent peak agrees quite well with observation at 504K (231 °C). The effect of water on the amide peak is calculated by scaling the model parameters for amide and water to predict a value of 250 K (see Supporting Information) to give a T_g gradient with humidity (%) of (491 − 250)/100 = 2.4, such that we will take a simple linear relation for effective T_g as a function of humidity with a form

$$T_g = 197 - 2.4H \ (°C) \quad (1)$$

which is an good fit to the experimental data right from the zero humidity point, as shown in Figure 2. Phrased in an alternative way, H can be quantified as a temperature change due to the increase in thermal energy of the water molecules, which have mobility that is quantified in GIM by an increase in the thermal degrees of freedom parameter.

The next step is to establish a reference profile for the temperature dependence of elastic modulus. Figure 4 compares the GIM predicted modulus profile with experimental DMA data at a frequency of 1 Hz, where the experimental DMA modulus has been calibrated against the tensile stress−strain value at 25 °C of 9.2 GPa. Since the two curves are reasonably close, we will use the model predictions for ease of calculation for purposes of demonstration. For reference, the predicted values of tensile modulus at 300 K and above T_g are 8.8 and 0.7 GPa, respectively, for a model *A. perni* silk with an ordered fraction of 0.5 (see Supporting Information).

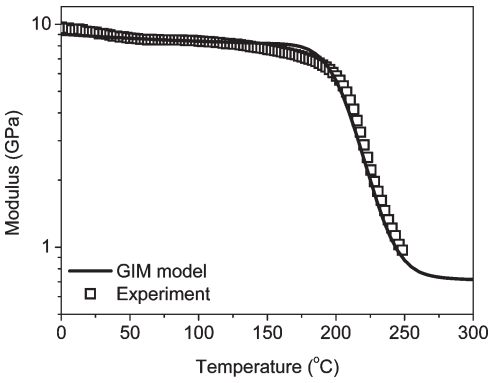

Figure 4. Experimental and predicted modulus−temperature profiles.

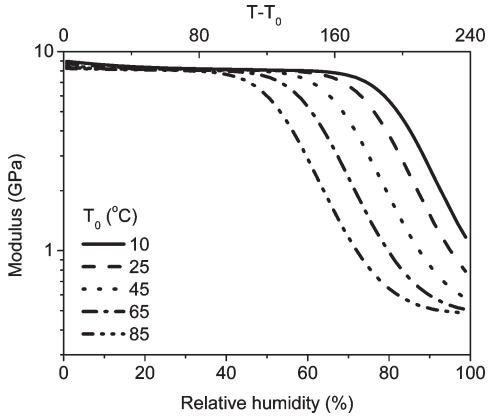

Figure 5. Simulations of modulus as a function of relative humidity at the same reference temperatures as shown in Figure 1B.

The experimental observations of modulus as a function of H in Figure 1B are taken at a series of reference temperatures, T_0. We now define H as a function of temperature from eq 1 in the form

$$H = \frac{T - T_0}{2.4} \tag{2}$$

Figure 5 replots the modulus-temperature profile from Figure 4 as modulus is a function of H for the same series of T_0 values. The simulated modulus profiles are in good general agreement with the observations shown in Figure 1B and suggest that treating humidity effectively as an increment of temperature in its effect on mechanical properties is reasonable and is potentially a very powerful and practical way to quantify humidity effects in proteins.

4. Conclusions

We have applied a new method to study the humidity dependence of *A. pernyi* silk's modulus at different temperatures. A linear relationship has been found between the glass transition temperature and the environment humidity which indicates the equivalence between increasing humidity and raising temperature in activating the glass transition of the silk. With that linear relationship, all five modulus−humidity curves are successfully included in a single modulus−($T_g - T$) master curve of *A. pernyi* silk with zero moisture. This humidity−temperature equivalence has been interpreted by means of group interaction modeling at the molecular level in terms of the contributions to the thermal energy in the protein due to temperature and extra degrees of freedom of relatively more mobile water molecules. This approach will be very valuable for understanding and predicting the effect of water on the mechanical properties of both natural proteins and synthetic polymers with hydrophilic groups.

Acknowledgment. This work was supported by the National Natural Science Foundation of China (NSFC 20525414) and the Programme for Changjiang Scholars and Innovative Research Team in the Fudan University as well as the AFOSR (F49620-03-1-0111) and the European Research Council (SP2-GA-2008-233409). The authors acknowledge the critical suggestions on the manuscript from professor Xin Chen and the kind help with obtaining the *A. pernyi* silkworms from Ruiwen Hao.

Supporting Information Available: SEM images of cross section of cryogenically fractured *A. pernyi* silk which was already contracted in water; details of predicting the dynamic mechanical spectrum, the stress−strain curve, and the humidity effects on the modulus of *A. pernyi* silk by group interaction modeling. This material is available free of charge via the Internet at http://pubs.acs.org.

References and Notes

(1) Yang, Y.; Chen, X.; Shao, Z. Z.; Zhou, P.; Porter, D.; Knight, D. P.; Vollrath, F. *Adv. Mater.* **2005**, *17*, 84–88.
(2) Shao, Z. Z.; Vollrath, F. *Nature* **2002**, *418*, 741–741.
(3) Shao, Z. Z.; Vollrath, F. *Polymer* **1999**, *40*, 1799–1806.
(4) Schafer, A.; Vehoff, T.; Glisovic, A.; Salditt, T. *Eur. Biophys. J. Biophys. Lett.* **2008**, *37*, 197–204.
(5) Vehoff, T.; Glisovic, A.; Schollmeyer, H.; Zippelius, A.; Salditt, T. *Biophys. J.* **2007**, *93*, 4425–4432.
(6) Perez-Rigueiro, J.; Viney, C.; Llorca, J.; Elices, M. *Polymer* **2000**, *41*, 8433–8439.
(7) Work, R. W.; Morosoff, N. *Text. Res. J.* **1982**, *52*, 349–356.
(8) Parkhe, A. D.; Seeley, S. K.; Gardner, K.; Thompson, L.; Lewis, R. V. *J. Mol. Recognit.* **1997**, *10*, 1–6.
(9) Yang, Z. T.; Liivak, O.; Seidel, A.; LaVerde, G.; Zax, D. B.; Jelinski, L. W. *J. Am. Chem. Soc.* **2000**, *122*, 9019–9025.
(10) Holland, G. P.; Lewis, R. V.; Yarger, J. L. *J. Am. Chem. Soc.* **2004**, *126*, 5867–5872.
(11) Hu, X.; Kaplan, D.; Cebe, P. *Thermochim. Acta* **2007**, *461*, 137–144.
(12) Agarwal, N.; Hoagland, D. A.; Farris, R. J. *J. Appl. Polym. Sci.* **1997**, *63*, 401−410.
(13) Plaza, G. R.; Guinea, G. V.; Perez-Rigueiro, J.; Elices, M. *J. Polym. Sci., Part B: Polym. Phys.* **2006**, *44*, 994–999.
(14) Park, Y.; Ko, J. Y.; Ahn, T. K.; Choe, S. *J. Polym. Sci., Part B: Polym. Phys.* **1997**, *35*, 807–815.
(15) Miri, V.; Persyn, O.; Lefebvre, J. M.; Seguela, R. *Eur. Polym. J.* **2009**, *45*, 757–762.
(16) Ellis, T. S.; Karasz, F. E. *Polymer* **1984**, *25*, 664–669.
(17) Tsukada, M.; Freddi, G.; Kasai, N.; Monti, P. *J. Polym. Sci., Part B: Polym. Phys.* **1998**, *36*, 2717–2724.
(18) Porter, D. *Group Interaction Modelling of Polymer Properties*; Marcel Dekker: New York, 1995.
(19) Porter, D.; Gould, P. J. *Int. J. Solids Struct.* **2009**, *46*, 1981–1993.
(20) Porter, D.; Vollrath, F.; Shao, Z. *Eur. Phys. J. E* **2005**, *16*, 199–206.
(21) Vollrath, F.; Porter, D. *Appl. Phys. A: Mater. Sci. Process.* **2006**, *82*, 205–212.
(22) Vollrath, F.; Porter, D. *Soft Matter* **2006**, *2*, 377–385.
(23) Porter, D.; Vollrath, F. *Soft Matter* **2008**, *4*, 328–336.